DYNAMIC INCREASE FACTOR
IN REINFORCED CONCRETE FRAMES
UNDER DISPROPORTIONATE COLLAPSE

A thesis presented to the Faculty of the Graduate School

at the University of Missouri – Columbia.

In partial fulfillment of the requirements for the degree

Master of Science

By

Joseph Ernest Kirby

Dr. Sarah L. Orton, Thesis Supervisor

May 2017

The undersigned, appointed by the dean of the Graduate School, have examined the thesis entitled:

DYNAMIC INCREASE FACTOR

IN REINFORCED CONCRETE FRAMES

UNDER DISPROPORTIONATE COLLAPSE

Presented by Joseph Ernest Kirby,

a candidate for the degree Master of Science,

and hereby certify that, in their opinion, it is worthy of acceptance.

_____

Professor Sarah Orton

_____

Professor Hani Salim

_____

Professor Sherif El-Gizawy

DEDICATION

This thesis is dedicated to my family (Ana Montoya, Rob Kirby, Frank Kirby and David Kirby), my girlfriend (Ana Kelty), my friends (Bryan Lightfoot, Ralph Agee, Greg Roberson and Andy Scott) and my thesis supervisor (Dr. Sarah Orton).

When I started this journey in 2010, I didn't appreciate the effort and self-discipline that would be required. At various times over these years, I've received support and guidance from everyone in this dedication. They've each shown me compassion, strength, and tough love when I needed it. Without them, this paper would not have been written.

ACKNOWLEDGEMENTS

I would like to express my gratitude to everyone at the University of Missouri – Columbia who contributed to this thesis. My professors (Dr. Sarah Orton, Dr. Hani Salim, Dr. Glenn Washer and Dr. Vellore Gopalaratnam) taught me the principles needed to understand this research, Richard Oberto provided his expertise to guarantee the accuracy of the data acquisition system, and my colleagues (Stephen Stinger, Aaron Saucier, Matthew Wombacher, Matthew Wheeler and Jeremiah Kasinger) provided their time, knowledge and sweat to develop, construct, setup and perform the test used for this study.

TABLE OF CONTENTS

LIST OF FIGURES

Page

LIST OF TABLES

Page

ABSTRACT

Under a disproportionate collapse, the sudden loss of a support causes a dynamic response that can amplify the internal forces in the surrounding members and lead to significant global damage. This study considered a two-dimensional, quarter scale, two bay, two story reinforced concrete frame with discontinuous reinforcement. In order to simulate an interior bay condition, the frame was axially restrained at the adjacent-bay beam locations. Dead weights were applied to simulate the dead and live loads expected to be present during a collapse event. To initiate the test, and to simulate the sudden loss of a load-bearing column, a kickstand was implemented. The results presented herein are from four dynamic tests under various levels of applied load. The fourth drop, with a load corresponding to 42% of the 1.2*DL + 0.5*LL typically specified in disproportionate collapse guidelines, resulted in a catenary action. The results show that there is a very fine tipping point at which the structure is pushed past the compressive arch and flexural range of resistance into the catenary action range (hereafter referred to as the snap-through effect). Furthermore, the results show that due to this snap-through effect, the dynamic increase factor can be as great as 2.4, significantly higher than the value specified by the aforementioned guidelines.

1 INTRODUCTION

Disproportionate collapse is defined as a situation where the local failure of a primary structural component leads to the collapse of adjoining members which, in turn, leads to additional collapse. Hence the total damage is disproportionate to the original cause (GSA, 2003). Causes of such a collapse include accidental loads (vehicle collisions, explosions from natural gas sources and mechanical equipment), construction errors, inadequate design, inadequate maintenance, extreme environmental events (earthquakes, tsunami waves, high-winds) and terrorist attacks. An example of a disproportionate collapse trigger in reinforced concrete structures is column punching shear failure in flat slabs floor systems due to inadequate detailing or corrosion of the reinforcement (Byfield et al., 2013). The sudden application of load on a new structural configuration, resulting from the instant loss of support, causes a dynamic reaction in the surrounding structure that can amplify the internal forces in the members. This leads to greater global damage than would have resulted from a static loading condition. Because the causes of such an event are relatively extreme and have unknown mean recurrence intervals, the vast majority of structures do not require consideration of disproportionate collapse design guidelines. However, the critical nature of disproportionate collapse and the potential harm to life warrant a study to better understand the behavior of a reinforced concrete structure in such an event. This in turn will allow structural engineers to implement efficient designs to mitigate the catastrophic damage in structures deemed susceptible by the code or client.

Generally, civilian structures are not designed for the abnormal loading conditions that may result in disproportionate collapse (NIST, 2007). This is because the additional capital required to design a structure for such abnormal conditions outweighs the probability of such an even occurring. This means the vast majority of existing structures are inherently susceptible. Another contributor of susceptibility results from improvements in structural design and analysis techniques. Modern structures are less conservative in design and consequently more vulnerable to unforeseen loading conditions (Smilowitz, 2006). When an unlikely loading event occurs, such as in the case of a disproportionate collapse, the injuries and loss of life can be severe, as was the case in the Oklahoma City bombing. If buildings could be designed with some inherent ability to withstand this type of collapse, then these losses would be limited. But to create such a design, practicing structural engineers need analysis methods that can predict the in-situ member forces resulting from a collapse scenario.

In order to accurately simulate the conditions of such a collapse, the selected analysis method must account for dynamic or inertial effects. The dynamic effects come from both the suddenly applied nature of the load, and the deformation of the structure until it reaches a resistance mechanism (discussed in the Literature Review section) capable of redistributing the member forces. To account for these inertial effects, a dynamic increase factor (DIF) is generally applied to the results of a static analysis. For this paper, a DIF is defined as the ratio of the static force on the structure (applied load) to the peak dynamic load the structure experiences (spring force); while a dynamic amplification factor (DAF) is the ratio of the peak response to the residual static response.

To aid in understanding the impact of inertial effects, consider a simple spring mass system (refer to Figure **1.1**). Assuming a spring with a linear stiffness constant (k) under a static load (P_o), the resulting deflection of the system would be u_{sto}. However, if the load was applied instantaneously, the resulting deflection of the system would be $2*u_{sto}$. Now consider that the load was applied with a specific rise time, somewhere between a static and instantaneous application. The resulting deflection would be something less than the scenario with an instantly applied load, and would depend on the ratio of the rise time to the natural period of the system. As seen in the figure, the peak response of a system with a rise time of $0.4*T_n$ is 84% of that of the instantly applied system. If the spring had a nonlinear resisting function, the deflection of the system would also depend on the ratio of the yield strength of the system (f_y) to the required resisting force of a corresponding linear system (f_o). The case for that with a ratio of 67% is plotted in Figure **1.1**, showing not only an increase in peak deflection of 32%, but also a permanent deflection. In this case, due to the nonlinear response of the spring, the force in the spring is only 1.25 times the applied load. Therefore, there is a lower equivalent dynamic increase factor for the nonlinear system. Although this sheds light on the significance of inertial effects on a simple spring mass system, the case of a reinforced concrete frame is significantly more complicated, since the nonlinear resisting function is not elastic-plastic.

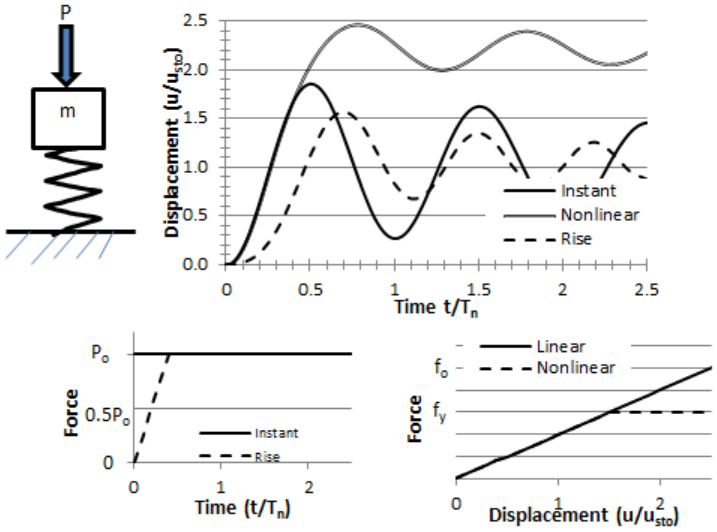

Figure 1.1: SDOF analysis of inelastic system under sudden load application

There are several analysis methods which are deemed suitable to account for inertial effects. In the second most common and simple analysis method, non-linear static analysis, a dynamic increase factor is applied to the factored design loads. However, there is limited empirical data obtained from dynamically loaded tests to justify the dynamic increase factors used in modern guidelines. Additionally, the quick nature of the loading may cause additional transient capacity in the resistance mechanisms which is not accounted for in the aforementioned factors.

1.1 Problem

At the time this experiment was performed, there was a limited amount of empirical data on the dynamic increase factor used for the disproportionate collapse of reinforced concrete structures. The purpose of this study is to experimentally evaluate the dynamic increase factor for reinforced concrete famed structures and investigate the consequences

of the snap-through effect. This understanding may lead to updates in the guidelines which will specify more accurate analysis techniques and more efficient resistance mechanisms for new structures, or more efficient retrofit procedures for existing structures. This will in turn allow our infrastructure to economically counteract disproportionate collapse.

1.2 Objectives and Research Approach

The primary objective of this research is to experimentally evaluate the dynamic increase factor of reinforced concrete framed structures. This dynamic increase factor serves as the only factor used to account for inertial effects in a non-linear static analysis, and is therefore critical to performing an accurate analysis. As part of this evaluation and serving as a secondary objective, the research will investigate the consequences of the snap-through effect on the response of the structure. Currently there is an absence of empirical data on the snap-through effect, which is experienced by every reinforced concrete frame structure that reaches the catenary action resistance mechanism. Furthermore, this research is primarily concerned with ductile failure modes (flexural and axial hinging) as Brunesi et al. (2015) found that both gravity only and seismically detailed reinforced concrete frames did not experience brittle shear failures.

This study considered a two-dimensional, quarter scale, two bay, two story reinforced concrete frame with discontinuous reinforcement, based on the 1971 ACI 318 code. A common structural system for existing office structures in low-seismic areas in the USA. To simulate an interior bay condition, the frame was axially restrained at the adjacent-bay

beam locations, approximately at the inflection points of the beams in a statically loaded condition. Dead weights were applied to simulate the dead and live loads expected to be present during a collapse event. To initiate the test, and to simulate the sudden loss of a load-bearing column, a kickstand was implemented. The frame was dynamically tested at four levels of applied load, up to a magnitude corresponding to 42% of the 1.2*DL + 0.5*LL typically specified in disproportionate collapse guidelines.

1.3 Outline

This research is organized into 6 chapters. Chapter 1 serves as an overview of the purpose and objectives of this research. Chapter 2 reviews historical examples of disproportionate collapse, discusses the primary resistance mechanisms (compressive arch action, Vierendeel action, and catenary action) in reinforced concrete structures, presents relevant research to illuminate what has been investigated and what requires additional study, and finally provides a summary of modern design guidelines used in the USA. Chapter 3 describes the experimental procedure, including the specimen's material properties, frame design and detailing, the physical test setup and instrumentation. Chapter 4 provides a raw presentation of the test results, discusses the equivalent dynamic amplification factors of various measures, and for greater understanding provides a single degree of freedom analysis comparison. Chapter 5 discusses topics and characteristics that require additional study, which arise because of the finite scope and resources for this research. Finally, Chapter 6 provides a comprehensive summary of the results and varies conclusions that have been drawn from this study.

2 LITERATURE REIVEW

To appreciate the importance of disproportionate collapse research, it is necessary to first review historical events which resulted from disproportionate collapse. These events will illustrate how the failure of a single structural element can caused a catastrophic global collapse which resulted in significant life and property loss. Afterwards, the structural mechanisms which resist disproportionate collapse will be identified and discussed, to aid in understanding the progression of resistance behavior. Next, previous research pertaining to disproportionate collapse of reinforced concrete structures will be presented. Finally, the chapter will conclude with a summary of modern guidelines used in the USA.

2.1 Historical Examples

One of the earliest cited disproportionate collapse events occurred in London, England in 1968. It involved the partial collapse of an apartment building called Ronan Point Tower (refer to Figure **2.1.1**). This building was 22-stories and constructed of pre-cast structural wall panels. The collapse was initiated by the failure of a wall panel near a corner on the 18th floor, which was destroyed by an accidental natural gas explosion. Because of the lack of redundancy in the joints between the wall panels and floor slabs, the impact from the loss of support of the upper floors caused a propagation of floor collapses to the ground. Four lives were lost and 17 injured. Fortunately, the event served as a catalyst for the development of new guidelines in England, including the Fifth Amendment to the Building Regulations in 1970. This regulation required that the removal of a single structural element would not cause a disproportionate collapse event (Pearson & Delatte, 2005).

Figure 2.1.1: Ronan Point Tower collapse (Pearson & Delatte, 2005)

Almost five years later (1973) another apartment building, this time with an attached parking structure, experienced a disproportionate collapse (refer to Figure **2.1.2**). The Skyline Center Complex, located in Bailey's Crossroads, Virginia, was designed to be 26-stories and constructed of cast-in-place columns with flat slab floor systems. The collapse occurred during construction, caused by the premature removal of shoring above the 22nd floor. Because the concrete hadn't reached adequate strength, the slab proved insufficient to support the 23rd floor columns and experienced punching shear failure. The collapse propagated to the ground and spread out to approximately 60 feet wide, resulting in 14 lives lost and 34 injured. Fortunately, the event influenced Fairfax County

to adopt a formal critical structures program where mandatory preconstruction meetings define temporary bracing requirements (Schellhammer et al., 2013).

Figure 2.1.2: Skyline Center Complex collapse (Schellhammer et al., 2013)

Unfortunately, several disproportionate collapse events were also caused by terrorist attacks, as was the case of the USA Marine barracks attack in Beirut, Lebanon in 1984 (refer to Figure **2.1.3**). The barracks was a 4-story reinforced concrete aviation administration building located at the Beirut International Airport. The collapse was caused by a vehicle-borne improvised explosive device (VBIED) whose explosion caused shear failures of the ground level columns. The blast lifted the building into the air, and when the structure impacted the ground, all floors collapsed on top of each other. The event resulted in 241 lives lost and more than 100 injured (Ernsberger Jr., 2016).

Figure 2.1.3: Beirut Marine barracks collapse (Ernsberger Jr., 2016)

Another construction related disproportionate collapse occurred in 1987 (refer to Figure **2.1.4**). L 'Ambiance Plaza, located in Bridgeport, Connecticut, was designed to be a 16-story apartment complex. The bottom 3-stories were to serve as a parking garage, and the entire building was constructed using the lift-slab method with post-tensioned floor slabs and steel columns. Approximately halfway through construction, three floor slab panels were lifted and placed at a temporary position in the west tower. Due to substandard welding at the slab-to-column connections, the panels fell, impacting the levels below, causing a collapse which propagated to the ground. The collapse also propagated east consuming the east tower, resulting in 28 lives lost (Martin and Delatte, 2000).

Figure 2.1.4: L ‘Ambiance Plaza collapse (Poisson, 2012)

Another disproportionate collapse caused by a VBIED occurred in 1995 (refer to Figure **2.1.5**). The Alfred P. Murrah federal building, located in Oklahoma City, was a 9-story reinforced concrete government complex. Because the columns were lightly reinforced, typical of low-seismic designs at the time, the blast loading from the VBIED caused adjacent columns to fail in shear. The lack of beam reinforcement continuity through the beam-column interface, coupled with the use of transfer girders to support every other perimeter column, rendered the structure helpless to redistribute the member forces from the destroyed columns. This initiated a disproportionate collapse which consumed almost half of the building and resulted in 168 lives lost (Corley et al., 1998).

Figure 2.1.5: Alfred P. Murrah federal building collapse (Jenkins, 2001)

Finally, a relatively recent and devastating event was the collapse of the World Trade Center towers in 2001 (refer to Figure **2.1.6**). The World Trade Center towers, located in New York City, were 110-stories and constructed of a complex structural system. Around the perimeter of the buildings, built-up tube columns were used to resist lateral loads as well as to support gravity loads. Floor loads were transferred to these columns via spandrel beams which connected the columns in groups of three. In the center of the buildings, a combination of build-up tube sections and wide-flange sections served as the columns to support gravity loads. Wide-flange beams transferred floor loads to the columns in the core area. To provide an open floorplan between the perimeter and core, open web steel joists with composite concrete floors were used to transfer floor loads and laterally brace the perimeter columns. Finally, from the 107th story to the roof, hat trusses were used to support roof loads. The collapse of each tower was caused by the

impact from a Boeing 767 liners, destroying up to 36 columns in the face of each tower. Due to the inherent redundancy in the design of the towers, specifically the hat trusses at the roof and the spandrel beams around the perimeter, the structures temporarily redistributed the member forces. Fires from burning fuel and office supplies continued to heat the structures and deteriorate the capacity of the columns until collapse began and propagated to the ground. The attack resulted in 2763 lives lost (Kirk, 2005).

Figure 2.1.6: World Trade Center collapse (McKee, 2010)

2.2 Resistance Mechanisms

When a critical structural element loses its ability to support load, the new structural configuration must redistribute the member forces to reach equilibrium and prevent a disproportionate collapse. However, the in-situ member forces which must be

redistributed are different from those of the undamaged structure, hence the new structural configuration. To study this difference in member forces, consider a four story, six bay structure with moment connections at every beam-column joist, as is typical with a cast-in-place reinforced concrete frame. Also, consider that an interior column on the ground level has been removed, as is the case for this research. A visual plot which compares the static major axis member moments of the undamaged and damaged structure is shown in Figure **2.2.1** (Orton, 2007). The figure shows that the negative beam moment at the columns surrounding the removed column has increased by almost a factor of 4. The positive beam moment has also increased but by a factor greater than 4, and peak magnitude is now located at the position of the removed column. This causes a moment reversal, requiring positive moment reinforcement where the beams were originally design for a negative moment. Unfortunately, greater beam moments and moment reversals are not the only member forces which must be redistributed. Axial loads, both compressive and tensile, dependent on the deflection, are also imposed on the damaged structure. In a reinforced concrete frame, the forces are redistributed via one of three resistance mechanisms: compressive arch action, Vierendeel action, and catenary action.

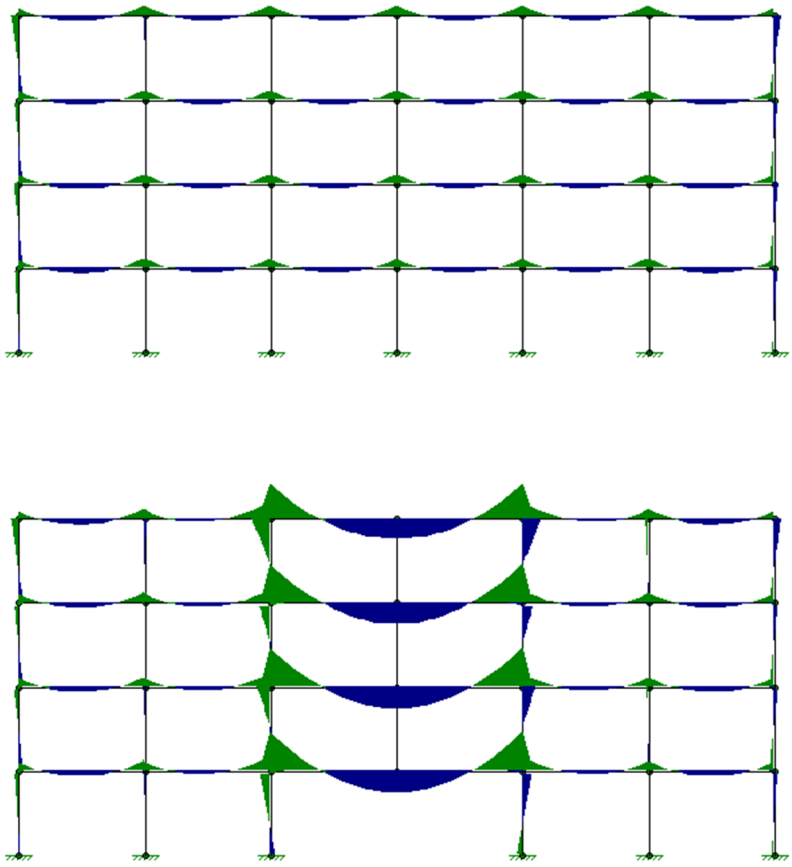

Figure 2.2.1: Static comparison of major axis moments due to column removal (Orton, 2007)

2.2.1 Compressive Arch Action

The resistance mechanism with its greatest contribution immediately following the loss of the structural element is compressive arch action. Similar to the response of a wall or deep beam, diagonal compressive struts form through the concrete from the top of the now double-span beam at the location of the removed column, to the bottom of the beam at each adjacent column support (refer to Figure **2.2.1.1**). The vertical components of these compressive struts allow the double-span beam to resist a relatively small amount of gravity load, while the horizontal components create a compressive force to be resisted

at the adjacent beam-column joints. As the beam deflects, the vertical component of the compressive struts decreases, therefore reducing the gravity capacity of the compressive arch action. Once the double-span beam reaches a deflection equal to its section depth, all compressive arch action resistance has been lost.

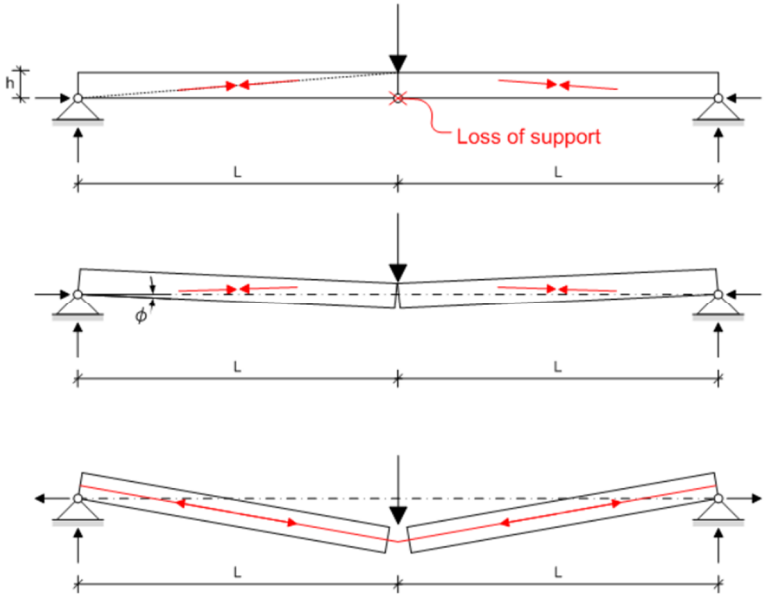

Figure 2.2.1.1: Catenary action phase (Couwenberg, 2013)

2.2.2 Vierendeel Action

During and following the compressive arch action phase, a flexural resistance mechanism also provides capacity to redistribute the member forces. This mechanism, known as Vierendeel action or frame action, resists the gravity loads through the moment connections at the remaining adjacent beam-column joints. Note that if a column(s) with tensile capacity remains above the location of the removed column, Vierendeel action will also be contributed by the upper level(s). If all the upper levels are loaded with identical in-situ loads at the time the column is removed, the additional contribution is

negligible. However, in the case of office buildings, the roof level is often loaded with significantly less load than the floor levels. Per the modern building codes, the roof level is often controlled by a 20psf live load to account for construction loads, or a snow load in cold-climate regions. This allows the Vierendeel action at the roof level to contribute additional resistance to the lower floors. The flexural resistance continues to redistribute the member forces until the double-span beam deflects sufficiently to crush the concrete at the compression blocks, therefore creating pins at the locations of the adjacent beam-column joints and the location of the removed column.

2.2.3 Catenary Action

As mentioned previously, once the double-span beam has deflected sufficiently, all compressive arch action resistance is lost. At this point, a "snap-through" effect occurs and another resistance mechanism is engaged, catenary action. Orton (2007) identified this "snap-through" transition and the fact that catenary action doesn't engage until the beam has reached a deflection equal to its section depth. Thus, the beam has deflected significantly and it can be assumed that hinges have formed at the midspan and supports. Depending on the flexural ductility of the double-span beam, there may be reserve flexural capacity. Therefore, hinge formation and true pin-pin-pin behavior may be a conservative assumption. Nonetheless, the hinges cause the double-span beam to act like a cable, causing tensile forces to develop. In the case of reinforced concrete frames, these tensile forces are developed through continuity of the beam's longitudinal reinforcement, either positive or negative. If the reinforcement is not continuous, as is the case for most existing structures in low-seismic areas, the tensile forces can transfer between the

beam's negative and positive longitudinal reinforcement via stirrups with sufficient spacing (refer to Figure **2.2.3.1**). These tensile forces allow the pseudo cable to resist the vertical forces acting on the double-span beam, the capacity of which increases as the deflection increases. This can be shown by analyzing a uniformly loaded simply supported beam with pinned end conditions (both horizontally restrained) and a pin at midspan (refer to Figure **2.2.3.2**). In order to maintain static equilibrium, the horizontal forces at the column supports (H) must equal the distributed load (q) * the double-span length squared (L^2) divided by the product of 8 and the deflection (delta). This is essentially the moment at midspan of a uniformly loaded simply supported beam (no hinge at midspan) divided by the deflection of the beam. This equation shows that if the applied distributed load remains constant, as the deflection of the double-span beam increases, the horizontal reactions at the supports decrease; hence, the capacity of the pseudo cable system increases.

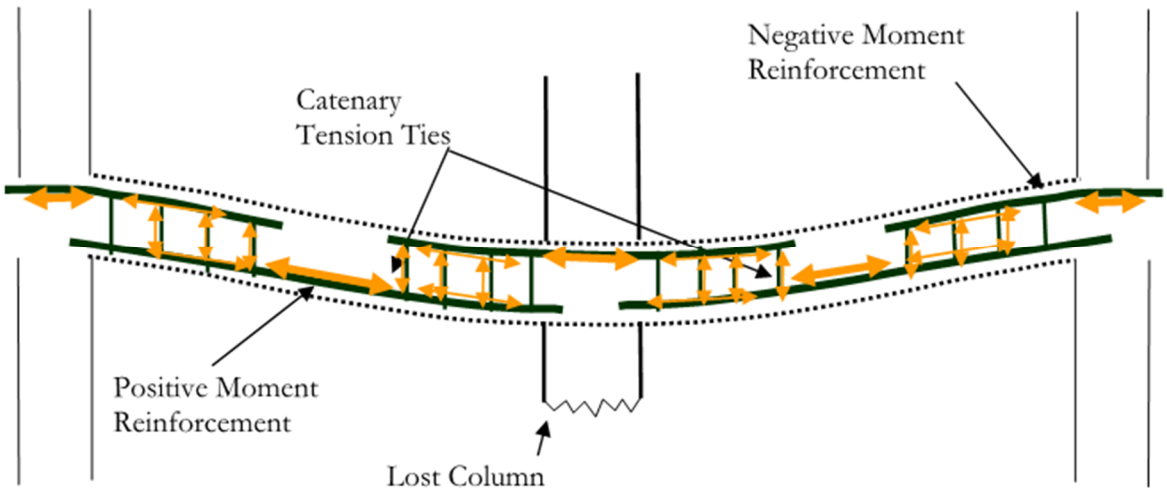

Figure 2.2.3.1: Catenary action tensile forces though stirrups (Orton, 2007)

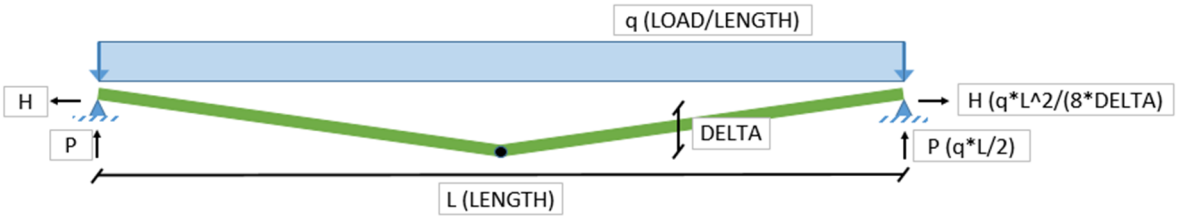

Figure 2.2.3.2: Uniformly loaded simply supported beam with hinge at midspan

When considering the global frame response, rather than that of an isolated beam, the behavior is similar to that mentioned in the Vierendeel action section. If a column(s) with tensile capacity remains above the location of the removed column, catenary action will also develop in the beams of the upper level(s) (refer to Figure **2.2.3.3**).

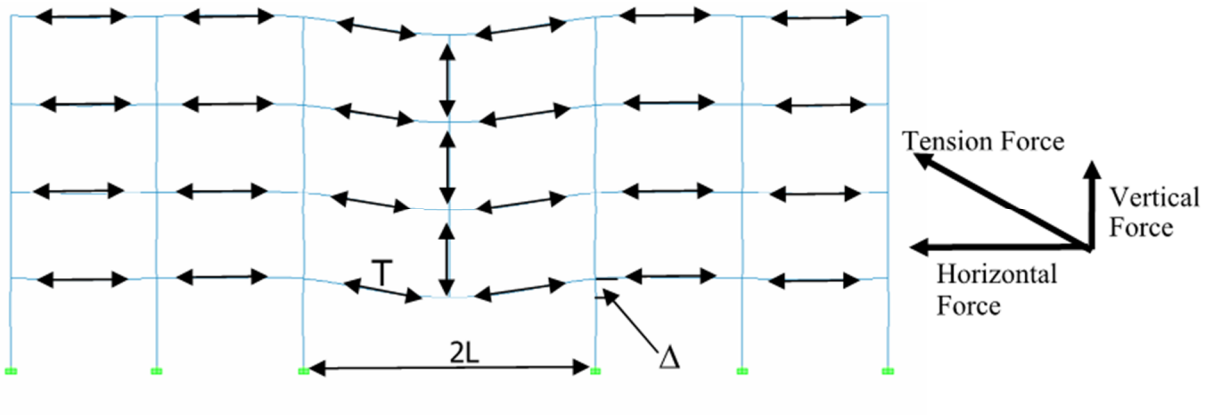

Figure 2.2.3.3: Catenary action tensile forces in a frame (Orton, 2007)

2.3 Previous Research

At the time this experiment was performed, there was a limited amount of empirical data on the dynamic increase factors used for the disproportionate collapse design of reinforced concrete structures. However, several studies have statically evaluated the

various resistance mechanisms and/or analyzed the resistance mechanisms using computational models. This chapter will discuss those studies in order to understand the foundation of modern disproportionate collapse guidelines.

One of the first studies on the disproportionate collapse resistance mechanisms of reinforced concrete buildings was presented in 1975. Following the Ronan Point Tower collapse, Regan (1975) performed statically loaded catenary tests on precast floor panels which simulated the loss of a center support (refer to Figure **2.3.1**). The tests were performed on 2 in thick panels of widths varying from 14 in to 28 in with a 2 in cast-in-place topping. The panels were supported with an 18 ft. span and a joint at midspan, the location of the pseudo removed support. Almost all of the specimens exhibited an initial compressive arch phase, followed by a sudden transition into the catenary action phase. While most of the panels failed via tear-out of the unyielded positive moment longitudinal reinforcement near the supports, some of the panels exhibited flexural yielding at these locations before failure. The latter specimens, which were able to definitively form hinges, achieved higher catenary loads and deflections than those with unyielded reinforcement. Regan concluded that ductility, and therefore detailing of the longitudinal reinforcement, is an important factor contributing to the catenary action capacity of precast panels.

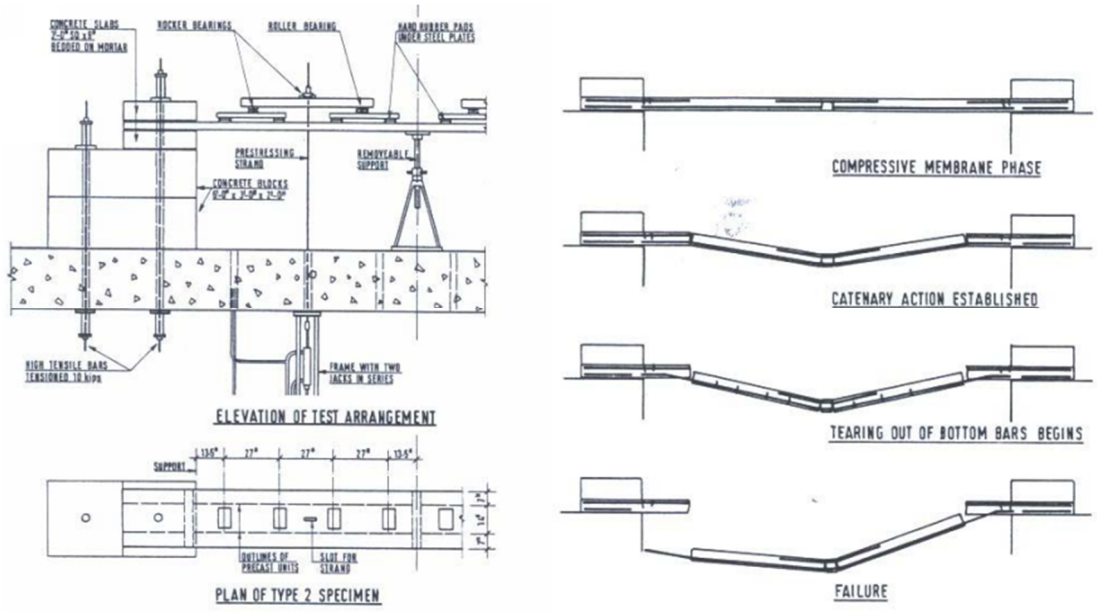

Figure 2.3.1: Catenary tests of precast floor panels (Regan, 1975)

Although various other studies were performed over the next few decades, it was the collapse of the World Trade Center towers that reignited interest in understanding the resistance mechanisms which would allow designers to mitigate disproportionate collapse. In 2007, Orton performed a study to develop retrofit procedures for reinforced concrete buildings, using carbon fiber reinforced polymers, with the intent of reducing vulnerability to such collapse. The study considered statically loaded two-dimensional, half scale reinforced concrete beams with continuous and discontinuous longitudinal reinforcement. The specimens were representative of a double-span continuous perimeter beam which loses support at an interior column due to a disproportionate collapse event (refer to Figure **2.3.2**). To gain insight into the resistance mechanisms inherent to reinforced concrete structures, tests were performed on non-retrofitted beams. From these tests Orton concluded that the catenary action phase of resistance begins after the beam has formed hinges and is unable to provide flexural resistance. Furthermore,

Orton concluded that the transition between resistance mechanisms is directly related to the height of the beam; therefore, catenary action doesn't engage until the beam has reached a deflection equal to the height of the member.

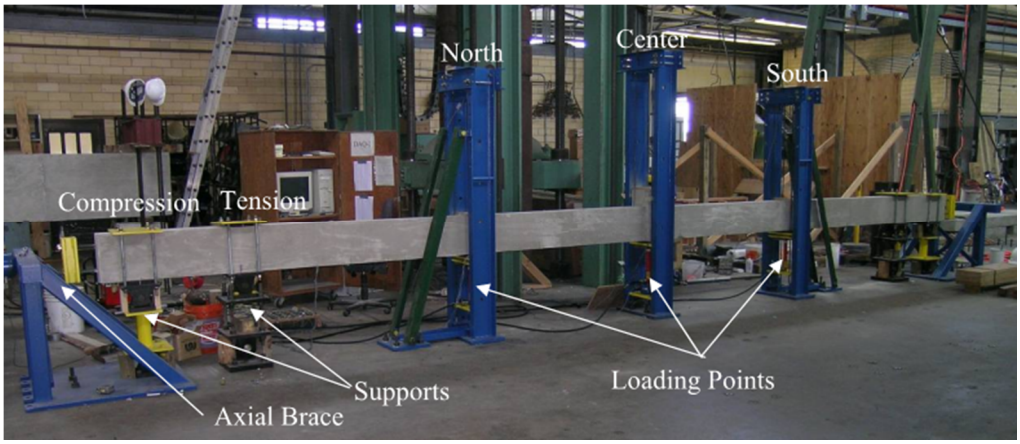

Figure 2.3.2: Photo of test setup (Orton, 2007)

The transition between resistance mechanism phases was later explicitly studied by Stinger in 2011 (refer to Figure **2.3.3**). The study considered three reinforced concrete frames, of different designs, under an instantaneous column loss event. The first frame was designed with discontinuous longitudinal reinforcement (identical to that in this study), the second was designed with continuous reinforcement, and the third was designed with discontinuous reinforcement but also included concrete masonry unit infill walls. The frames were statically loaded at the location of the removed column. Considering the frame with continuous reinforcement, the results show that the initial resistance mechanisms were flexural action and compressive arch action. As the frame deflected, hinges formed at the adjacent column supports and above the removed column. These mechanisms continued to provide resistance until the longitudinal reinforcement in

tension fractured. At this point the frame transitioned to the catenary action phase. Regarding the frame with discontinuous reinforcement, the results show that the initial resistance mechanism was compressive arch action. This mechanism continued to provide resistance until the beam reached a deflection equal to its depth. At this point the frame transition to the catenary action phase. It is interesting to note that both the continuous and discontinuous frames exhibited nearly identical magnitudes of resistance due to catenary action. Tests by other researchers have also shown these typical load deflection behaviors for reinforced concrete frames [Sasani (2008a), Yi et al. (2008), He and Yi (2008), Bazan (2008), Orton et al. (2009) and Su et al. (2009)]. However, the aforementioned studies did not investigate the effect of the dynamic application of load on the phase transition into catenary action.

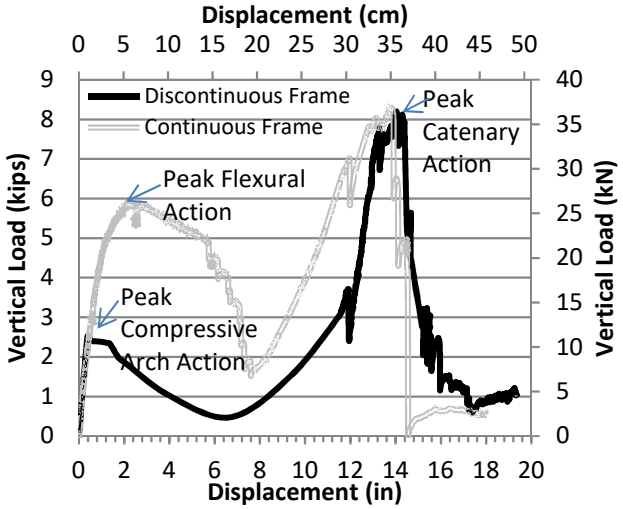

Figure 2.3.3: Load deflection results from static tests (Stinger, 2011)

There have been a limited number of tests that experimentally evaluated the disproportionate collapse response of reinforced concrete frames under dynamic loading.

One of those tests was presented by Tian and Su in 2011. The study evaluated the dynamic response of four axially restrained, two-dimensional, full scale, double-span beams with continuous reinforcement. The goal of the research was to determine the collapse resistance contribution of compressive arch action. The beams were loaded with dead weights and the center support suddenly removed to initiate the response. The results show that the ratio of peak dynamic moment to static moment ranged from 1.7 to 1.36, depending on the level of load. Beams with higher levels of load saw reduced DIFs due to decreased stiffness at the higher loads.

Another study that incorporated dynamic loads into the test was presented by Sasani et al. in 2007. The study involved a two-dimensional, eighth scale, four bay, three story reinforced concrete frame with continuous reinforcement. The frame was loaded with dead weights, and to initiate the test, the center lower column suddenly broken. The frame experienced a peak deflection of only 0.55 cm (0.22 in) and a residual deflection of 0.50 cm (0.2 in)

There have been a few studies that involved the dynamic testing of three dimensional frames, accounting for the contribution of secondary beams and floor slabs. Sasani et al. (2008b, 2010) studied the disproportionate collapse potential of existing reinforced concrete buildings, with infill wall panels, slated for demolition. The buildings experienced the removal of multiple columns at various exterior and interior locations. These studies found that Vierendeel action, in conjunction with increased stiffness from infill wall panels and continuity with the floor slabs and secondary beams, contributed

significantly to resisting collapse. It is interesting to note that all of the buildings in these studies were able to successfully redistribute the loads, therefore avoiding disproportionate collapse and even significant residual displacement.

However, with so few experimental tests, most of the criteria used to determine dynamic increase factors is based on modern design philosophies and analytical data. The factors used in the Department of Defense's Uniform Facilities Criteria guideline are calculated from equations based primarily on the work of McKay et al. (2007). To determine the DIFs for reinforced concrete buildings, McKay et al. used a structural analysis program which incorporated hinges, the properties of which were defined according to FEMA 356. It is important to note that the models did not consider the response of compressive arch action or catenary action in the beams. The dynamic increase factors determined from the models of various reinforced concrete buildings ranged from 1.4 to 1.05, and the beams with the greatest inherent rotational ductility exhibited the lowest DIFs. Tsai (2011) also studied the DIFs for reinforced concrete buildings and determined an analytical equation to predict the factor based on a linear-plastic load displacement relationship. The results from Tsai were similar to those from McKay et al., but this research also concluded that the DIF was larger for highly ductile buildings if a positive post-yield stiffness was incorporated into the analysis.

2.4 Guidelines

The first disproportionate collapse guidelines were developed in England following the collapse of the Ronan Point Tower. The Fifth Amendment of the Building Regulations

was created in 1970 and required that the removal of a single structural element would not cause a disproportionate collapse event (Pearson & Delatte, 2005). Although several professional design organizations (including ACI and ASCE) created provisions over the following years that involved general structural integrity to mitigate such a collapse, official provisions were not created by U.S.A. government agencies until after the turn of the millenium. In 2003 and 2004, the General Services Administration (GSA) and the Department of Defense (DoD) created disproportionate collapse provisions, respectively. The purpose of these provisions was to "provide the design requirements necessary to reduce the potential of progressive collapse for new and existing facilities that experience localized structural damage through normally unforeseeable events" (DoD, 2004).

Both guidelines identify two methods to provide disproportionate collapse resistance, an Indirect method and a Direct method. The Indirect method was developed from the aftermath of the Ronan Point Tower collapse, and involves the use of prescriptive design rules which require minimum levels of strength and continuity throughout the structure. Continuity is achieved with tension ties that enable catenary action (with sufficient deflection) therefore allowing the surrounding structure to redistribute loads from a damaged structural element (refer to Figure **2.4.1**). The Direct method requires analysis of the structure subjected to a disproportionate collapse event, and can be categorized into two approaches: Active and Passive. The Active approach mitigates collapse potential by using non-structural elements to reduce the probability that an event damages the structure, and through the identification and design of critical structural elements to retain capacity after an event (i.e. Enhanced Local Resistance). The Passive approach of the

Direct Method involves the assumption that a critical structural element has failed, and the new structural system must use alternate load paths to redistribute the loads (i.e. Alternate Load Path). This approach may also involve isolation by segmentation, in which the potential extent of collapse is limited to a predefined area by isolating different structural systems within the building, therefore preventing a global collapse.

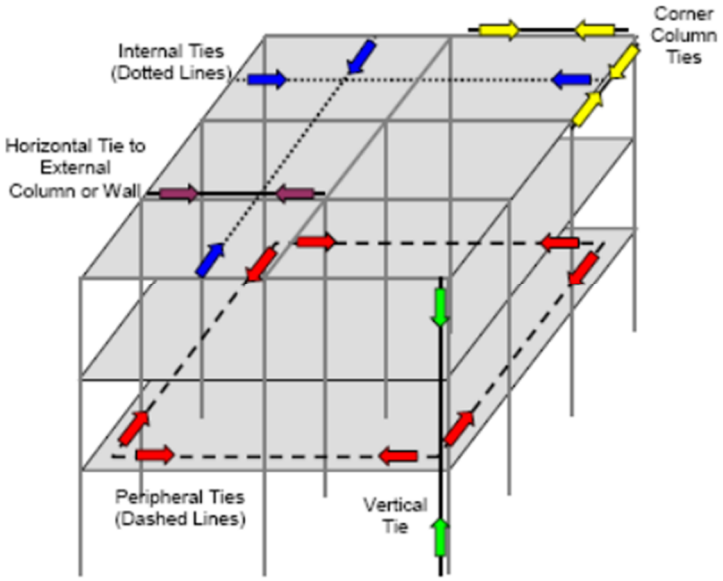

Figure 2.4.1: System of tie forces (DoD, 2004)

To perform the analysis required by the Alternate Load Path method, both the GSA and DoD guidelines specify several accepted analysis methods; they are linear static (LS), nonlinear static (NS) and nonlinear dynamic (ND) analyses. A linear dynamic analysis method is not presented in either guideline because the structural elements must remain elastic during the analysis. This is obviously difficult to maintain, since the structure will deflect significantly under dynamic loads and will invariably experience inelastic deformations.

Regarding the acceptable analysis methods, a LS analysis is the most common and simple choice. However, it also produces the most conservative and therefore least economical designs. To account for inertial and inelasticity effects which are not inherently incorporated into the analysis, a dynamic amplification factor is applied to the design loads. This factor amplifies the static loads to a magnitude which will supposedly produce pseudo member force and deflection results equivalent to those which would have been calculated from a dynamic analysis. Both the DoD and the GSA guidelines specify a factor of 2.0, however some studies have shown that this factor may be overly conservative (Ruth et al., 2006).

The second most common analysis method is a NS analysis. Although this analysis method is more complicated than a LS analysis, the results are more economical because inelastic material behavior is inherently incorporated into the analysis. Therefore, inertial effects are the only consideration not accounted for. To do so, a dynamic increase factor amplifies the static loads to a magnitude which will produce a pseudo response equivalent to that of a dynamic analysis. The GSA guideline and the 2005 DoD guideline specify a DIF of 2.0 for a NS analysis. However, the current DoD guideline (2009) specify the DIF as a function of the member ductility ($\theta pra/\theta y$), the function of which is based on the material and structural system types. For reinforced concrete beams, θpra is the plastic rotation angle given in the acceptance criteria and θy is the yield rotation angle using effective stiffness values in ASCE 41. For the DIF function associated with reinforced concrete framed structures, refer to Table **2.4.1**. The acceptance criteria

suggested in the DoD guideline for the plastic rotation angle is primarily based on the ASCE 41 provisions for seismic evaluation and rehabilitation. Because of the difference in loading conditions between disproportionate collapse and seismic events, using data from seismic tests to extrapolate the inelastic deformation capacity has been controversial. A recent study reported to the ASCE Disproportionate Collapse Standards and Guidance (DCSG) Committee found that exceeding ASCE 41 rotation limits does not necessarily lead to a disproportionate collapse. Additionally, a rotational ductility can only be found for sections that have tension reinforcement. In the case of beams with discontinuous steel, hinges will form in sections of discontinuity (where there is no tension steel) making it impossible to determine the DIF. Therefore, although a NS analysis is an economical choice, it is not without fault.

Table 2.4.1: Nonlinear static load combinations

Code	**Nonlinear Static Load Combination**
UFC (2005):	2*[(0.9 or 1.2)*DL + (0.5*LL or 0.2*SL)]
UFC (2009):	Ω_N*[(0.9 or 1.2)*DL + (0.5*LL or 0.2*SL)]
GSA:	2*(DL + 0.25*LL)

$\Omega_N = 1.04 + [0.45 / (\theta pra/\theta y + 0.48)]$

The final acceptable analysis method is a ND analysis. This method is the most accurate choice (Marjanishvili et al. 2006) but is also the most complicated procedure. The difficulty arises from the need to accurately represent the nonlinear resisting function which results from the transition into the catenary action phase. Therefore, ND analysis

is generally only performed in academic environments and deemed too complicated for code implementation.

3 EXPERIMENTAL PROCEDURE

This study considered a two-dimensional, quarter scale, two bay, two story reinforced concrete frame with discontinuous reinforcement. This chapter will first outline the properties of the concrete and steel used to construct the frame. Next, the prototype structure's design, on which the specimen is based, will be discussed. The section following will discuss the reaction frame used to simulate the interaction with the remainder of the structure, the kickstand used to simulate the sudden removal of a column, and the application of weight used to simulate the design loads. The chapter will finish with a discussion of the measuring devices and data acquisition system.

3.1 Material Properties

Material properties were determined according to the American Society of Testing and Materials (ASTM) standards (refer to Table **3.1.1**). Concrete cylinder compression tests were performed according to ASTM C39. The concrete was supplied by a local ready mix company with a maximum aggregate size of 1 cm (3/8 in) and specified concrete strength of 27.5 MPa (4000 psi). Although the concrete was specified with a compressive strength of 4000 psi, at the time of the dynamic test, the cylinder specimen exhibited a strength of 43.1 MPa (6271 psi). Reinforcement tension tests were performed according to ASTM A370. The #3 bar, specified with a tensile yield strength of 412 MPa (60,000 psi), exhibited a strength of 399 MPa (58,000 psi). The #2 bar, specified with a tensile yield strength of 619 MPa (90,000 psi), exhibited a strength of 565 MPa (82,000 psi).

Table 3.1.1: Concrete and steel material properties

Property	Value
Concrete Compressive Strength	6271 psi (43.2MPa)
#3 reinforcing bar	
yield	58 ksi (399 MPa)
ultimate	94 ksi (648 MPa)
strain at fracture	0.2 in/in
#2 reinforcing bar	
yield	82 ksi (565 MPa)
ultimate	95 ksi (655 MPa)
strain at fracture	0.12 in/in

3.2 Specimen Design and Construction

The prototype structure is six bays long and three bays wide, with 7.3 m (24 feet) bay spacing in both directions, and six levels tall with 3.6 m (12 feet) story heights. The specimen represents a two-dimensional, quarter scale section of two bays and two stories from the interior of the long side of the building perimeter (Figure **3.2.1**). For this study, secondary beam action and continuity from the floor slabs were not considered. The center column of the specimen represents the critical structural element that is assumed damaged for the alternate load path analysis.

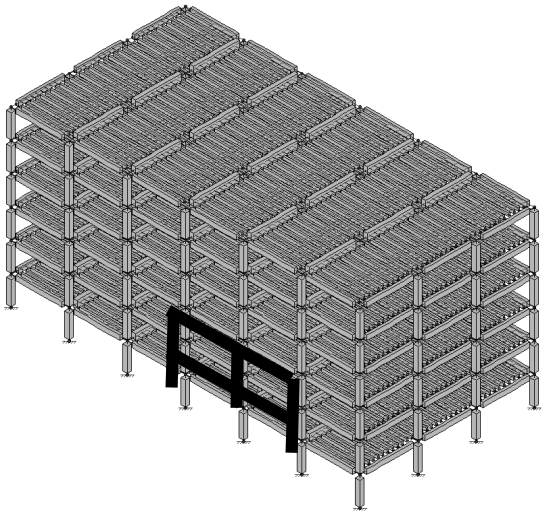

Figure 3.2.1: Relationship of test specimen to prototype structure

The reinforcement design of the test specimen is shown in Figure **3.2.2**. To simulate a design that is typical of existing reinforced concrete buildings in low seismic areas, the reinforcement was designed and detailed per the 1971 edition of the ACI 318 building code. The beams were designed with discontinuous longitudinal reinforcement; therefore, the positive moment reinforcement was discontinuous at all column supports and the negative moment reinforcement was discontinuous at each midspan. The maximum negative moment reinforcement consisted of four #2 bars [6.3 mm (1/4 in) diameter] and the maximum positive moment reinforcement consisted of three #2 bars. Unfortunately, the manufacturing process of small diameter bars can decrease in their ductility. Therefore, the bars were annealed to increase their ductility to that found in typical rebar. The beam transverse reinforcement consisted of W2 smooth wires spaced at 3.8 cm (1.5 in). These stirrups had 90-degree lap splices at the top, as is typical of older construction.

Figure 3.2.2: Reinforcement design of test specimen (1in = 25.4 mm)

3.3 Test Setup

The specimen was designed with connections to a reaction frame which simulated the interaction with the remainder of the structure. This reaction frame was designed to provide sufficient horizontal restraint to simulate the stiffness of the surrounding prototype structure. Based on computational analysis, this stiffness was determined to be 2200 kN/cm (1250 kip/in). Figure **3.3.1** shows the design of the reaction frame and the connections to the specimen. The columns of the specimen were supported by concrete pedestals attached to the loading floor, which provided moment resistance at the base of the columns. To allow for a disproportionate collapse simulation, the center column of the specimen was not supported. A collar apparatus attached to the unsupported column provided out-of-plane translation resistance in two directions while allowing for

uninhibited vertical deflection. The collar apparatus was attached to the reaction frame via linear ball bearings that slid along a clean high-strength steel rail (refer to Figure **3.3.2**).

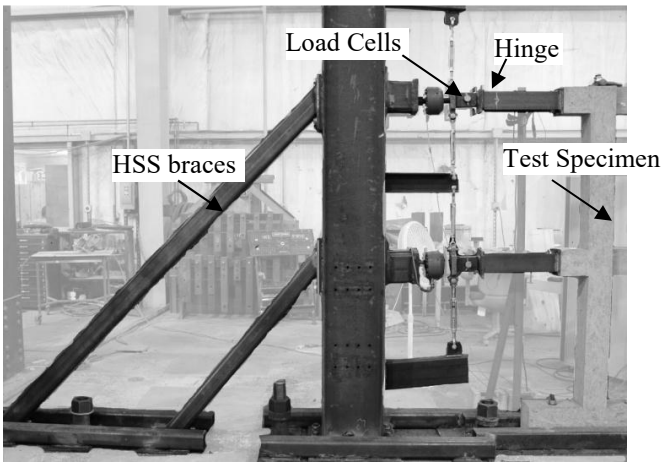

Figure 3.3.1: Reaction frame

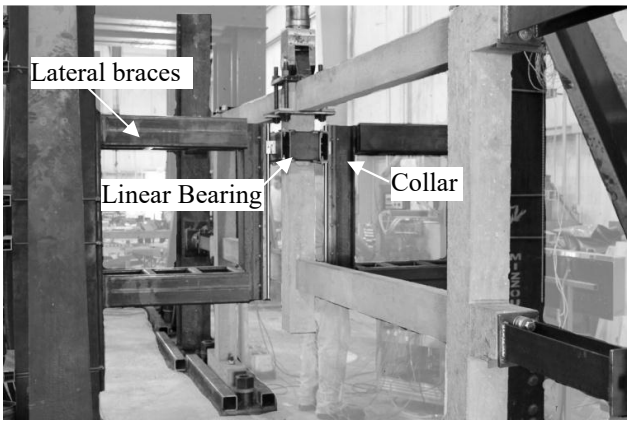

Figure 3.3.2: Collar for the center column

Gudmundsson and Izzuddin (2010) determined that an instantaneous column loss scenario is a viable way to study the disproportionate collapse resistance of a structure. Various methods on how to initiate the test were theorized, and a kickstand was

determined to be the simplest way to achieve near instantaneous column removal (refer to Figure **3.3.3)**. The kickstand was constructed from wood and placed directly beneath the pseudo damaged column. A notch was cut in the center of the kickstand so that when a lateral load was applied, the stand would buckle. To prevent premature failure, the kickstand was fitted with a collar which prevented it from buckling while in position. To further prevent premature failure, additional gravity supports (two 2x4s and two additional kickstands) were placed underneath the lower beams framing into the pseudo damaged column. These additional supports were designed to remain unloaded, however become immediately engaged should the primary kickstand buckle prematurely. To initiate a test, the secondary supports were first removed, followed by the collar on the primary kickstand. Once free, the primary kickstand was impacted at the notched part of the stand, causing it to buckle.

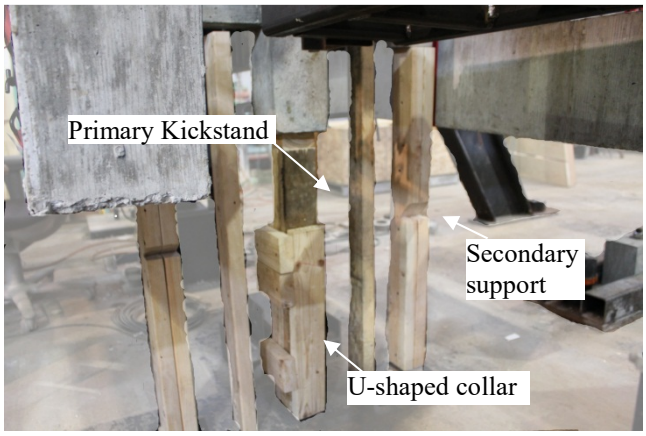

Figure 3.3.3: Kickstand

To simulate the dead and live loads required by design, dead weights were applied to the upper and lower beams of the frame. According to UFC guidelines, the beams were

required to carry a load combination of 1.2*DL + 0.5*LL without failure to satisfy collapse resistance. This load corresponds to a total additional weight of 57 kN (13 kips) on the frame. Based on the sister research project performed by Stinger (2011), the UFC design load combination was deemed too great. It was decided to start testing at a load corresponding to approximately half of the peak value measured in the statically loaded frame of Stinger (2011), or 14kN (3.2 kip). If this load was sufficient to push the frame past the compressive arch phase and into the catenary action phase, it would correspond to a dynamic increase factor of 2.0.

Dead weight was applied to the frame with reinforced concrete blocks and steel sections. The weight was distributed at quarter-points along the single-bay clear-span of each beam to mimic the distributed gravity loads present in the prototype structure. Refer to Figure **3.3.4** for a schematic of the weight distribution on the scaled frame. The concrete blocks were 144 x 23 x 15 cm (57 x 9 x 6 in) reinforced concrete beams each weighting approximately 1.2 kN (270 lbs). Each block weight was attached beneath the beams of the scaled frame using two tie-downs straps. Wood wedges were inserted between the bottom of the scaled frame beams and the top of the block weights to maximize the tension in the tie-down straps and ensure that the block would not rotate relative to the scaled frame during the collapse event.

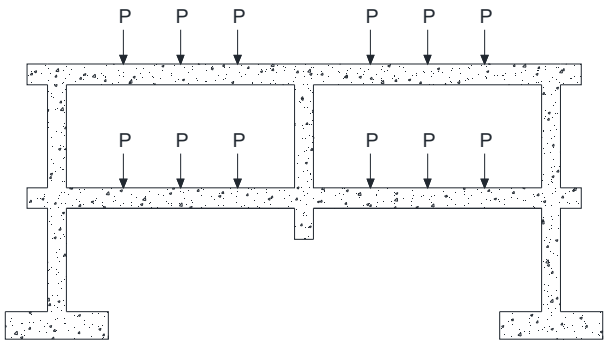

Figure 3.3.4: Application of weight

After the first drop, the frame did not exhibit significant damage. Therefore, three additional drops, each with an increasing amount of weight, were performed to reach the catenary action phase of response. To apply additional load, metal sections and 0.22 kN (50 lbs) lead weights were attached to the block weights. Care was given to ensure the additional weight was applied to retain the initial quarter-point distribution. Table **3.3.1** shows the total applied weight for each drop.

Table 3.3.1: Applied weights

Drop	Additional weight	Total Weight
1	-	*3238 lbs (14403 N)*
2	-	*3238 lbs (14403N)*
3	*1491 lbs (6632 N)*	*4729 lbs (21035 N)*
4	*794 lbs (3531 N)*	*5523 lbs (24567 N)*

3.4 Instrumentation

The test specimen was fitted with instrumentation to record the dynamic test. Horizontal load cells were placed in between the steel reaction frame and test specimen on one side

of the scaled frame (Refer to Figure **3.3.1**). Their purpose was to measure the compressive arch and catenary tension forces transferred to the remainder of the structure. Two LVDTs were placed on the test specimen column adjacent to the load cells to measure the beam level horizontal deflection of the test frame. Strain gages were placed at locations of expected significant moment (at the ends and centers of the beams) as well as at several other locations to record the strains in the reinforcement. A string-pot was placed beneath the pseudo damaged column to measure the peak dynamic and resting vertical deflections. Finally, an accelerometer was placed above the pseudo damaged column to measure the inertial effects.

To record the readings from the instrumentation in real-time, a data acquisition system was setup with a sampling rate of 500 samples per second. Due to the inevitable noise generated at such a high sampling rate, a 10-tap non-recursive low-pass finite impulse response filter was applied to the data in Excel. The instruments were arranged in order of increasing signal range, to minimize signal bleed from one channel to the next. The load cells and strain gages operated within a range of +1 V to -1 V, while the string-pot, LVDTs and accelerometer operated within a range of +10 V to -10 V. The noise in the signal was ± 0.004 V for the ± 1V channels and ± 0.004V for the ±10 V channels. This led to a post-filtering noise of ±0.00002 strain in the strain gages, ±0.45 kN (0.1 kip) in the load cells, ±0.005 mm (0.0002 in) in the LVDTs, and ±0.12 mm (0.007 in) in the string pot.

4 EXPERIMENTAL RESULTS AND DISCUSSION

4.1 Test Results

Static Test

Prior to the dynamic test performed for this study, a static test was performed on a frame of the same design. The load displacement results for this "sister" frame are shown in Figure **2.3.3** and complete information about the test results can be found in Stinger (2011). As loading began, due to the axial restraints at the beams, the frame experienced a compressive arch phase. As loading continued, the frame began to crack at the ends of the discontinuous reinforcement [55 cm (21.5 in) from the outer columns and on both sides of the center column]. This cracking created "beam blocks" the ends of which formed hinges. As the beam blocks rotated, high stresses were introduced at the corners which eventually lead to crushing of the concrete and loss of the compressive arch resistance. At this point the load carried by the frame dropped significantly to near 0 until about 17 cm (6.70 in) of displacement. At this point catenary action began to provide resistance which induced tensile stresses in the beams. At the end of the catenary action phase, the frame reached a maximum vertical load of 36.4 kN (8.19 kips). The final failure of the frame occurred when the negative moment reinforcement ripped out of the stirrups near the location of the center column.

Dynamic Tests

Four drop tests were conducted with applied weights as described in Table **3.3.1**. The first drop consisted of an applied weight of 14.4 kN (3238 lbs). This load corresponds to 25% the 1.2*DL + 0.5*LL required by the UFC guidelines. This weight was originally

thought to be sufficient to damage the specimen beyond the compressive arch phase. When the drop was conducted, the line to the string pot was snapped by the kickstand; therefore no displacement data is available for this drop. Peak and static values for the horizontal load cells, LVDTs, and accelerometer are available in Table **4.1.1**. Due to the small amount of load on the frame, values for the horizontal load cells were not greater than the noise in the signal [±0.45 kN (0.1 kip)], therefore no values are given for those readings. After the drop, the residual displacement of the center column of the frame was measured to be 0.5 cm (0.2 in). The relatively minor amount of movement indicated that the frame resisted the load entirely through compressive arch action.

Table 4.1.1: Test results

		Drop 1	**Drop 2**	**Drop 3**	**Drop 4**
Vertical Disp. (in)	Peak	-	0.54 in (1.37 cm)	1.34 in (3.40 cm)	12.92 in (32.82 cm)
	Static	-	0.50 in (1.20 cm)	1.20 in (3.05 cm)	11.89 in (30.20 cm)
Horiz. Disp. on top beam	Peak	0.022 in (0.06 cm)	0.0637 in (0.16 cm)	0.1640 in (0.42 cm)	-0.4333 in (-1.10 cm)
	Static	0.0211 in (0.05 cm)	0.0584 in (0.15 cm	0.1570 in (0.040 cm)	-0.3007 in (-0.76 cm)
Horiz. Disp. On bottom beam	Peak	0.0035 in (0.01 cm)	0.0230 in (0.06 cm)	0.0578 in (0.15 cm)	-0.1818 in (-0.46 cm)
	Static	0.0029 in (0.01 cm)	0.0208 in (0.05 cm)	0.0527 in (0.13 cm)	-0.1244 in (-0.32 cm)
Horiz. Load on bottom beam	Peak	-	-	0.3 kip (1.33kN)	-3.46 kip (-15.39 kN)
	Static	-	-	-	-0.77 kip (-3.42 kN)
Horiz. load on top beam	Peak	-	-	1.81 kip (8.05 kN)	-9.74 kip (-43.32 kN)
	Static	-	-	0.99 kip (4.40 kN)	-4.46 kip (-19.83 kN)
Acceleration	Peak	0.95 g	1.86 g	4.85 g	13.07 g

To attain displacement data, a second drop was conducted at the same applied weight. Although, the frame was reset to the same original position, the damage caused by the first drop was preexisting. Energy absorption due to concrete cracking in tension areas

and concrete crushing in compression areas would not be available in the second drop as it was in the first. Therefore, the second drop would be expected to have a greater level of damage and displacements. The time displacement history of the drop is given in Figure **4.1.1** and other important data is presented in Table **4.1.1**. As seen in Figure **4.1.1** the frame reached a peak displacement of 1.37 cm (0.54 in) and a residual displacement of 1.27 cm (0.5 in); therefore, exhibiting a residual displacement greater than in the first drop. Although this displacement was still within the compressive arch action range of the response, it was nearly twice that of the first drop due to the preexisting damage in the beam. This illustrates the potential effect of preexisting damage on the test, and warrants further research to verify the results collected in this study.

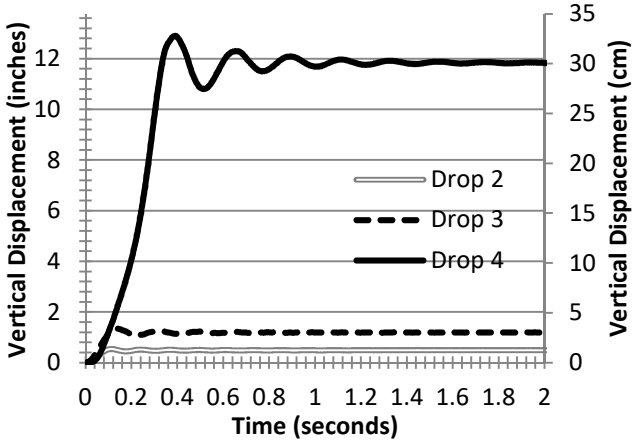

Figure 4.1.1: Time displacement history of drop tests

For the third drop the frame was reset to the original position, and an additional 6.3 kN (1491 lbs) of load was added for a total of 21 kN (4729 lbs) or 36% of the load 1.2*DL +0.5*LL distributed load on the beam. The time displacement history of the drop is given in Figure **4.1.1** and other important data is presented in Table **4.1.1**. As seen in

Figure **4.1.1** the frame reached a peak displacement of 3.4 cm (1.34 in) and a residual displacement of 3.05 cm (1.20 in). Again, this displacement was still within the compressive arch action range of the response. A picture of the specimen after the drop shown in Figure **4.1.2** illustrates the lack of significant damage at this level of load.

Figure 4.1.2: Frame after third drop

For the fourth drop, an additional 3.5 kN (795 lbs) was added for a total of 24.6 kN (5524 lbs) of load distributed on the frame. This load corresponds to 42% of the 1.2*DL +0.5*LL distributed load on the frame. The data presented in Figure **4.1.1** and Table **4.1.1** shows that this drop caused a significant amount of damage to the specimen and pushed the frame beyond the compressive arch range of response into the catenary action phase. The peak displacement of the frame was 32.8 cm (12.92 in) and the residual displacement was 30.2 cm (11.89 in). Readings from the horizontal LVDTs and load cells are given in Figure **4.1.3**. As seen in the figure, there is an initial compressive reaction that is then transferred into a tensile reaction. The peak tensile reaction of the specimen was 43.3 kN (9.74 kips), or just less than twice the applied load. To reach a

catenary action range of response, the surrounding structure needs to be able to transfer this level of load. The readings given by strain gages show strains close to or above yield throughout the top and bottom reinforcement. Again, the strain gages indicate the high level of tension throughout the beams of the specimen. The tension is carried by the negative moment reinforcement next to the column and transferred to the positive moment reinforcement toward the center of the beam. The final state of the frame is shown in Figure **4.1.4**. Although the frame is significantly damaged, the frame is still carrying its load and shows that catenary action is a possible way to arrest a collapse.

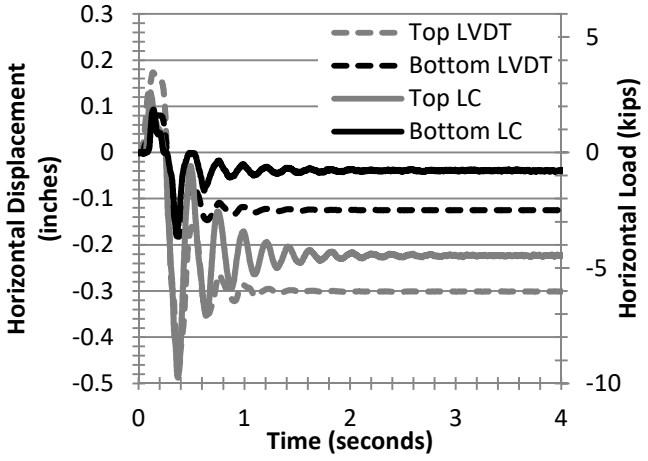

Figure 4.1.3: Horizontal load and displacement data from fourth drop (1 kip= 4.448 kN, 1in = 25.4 mm)

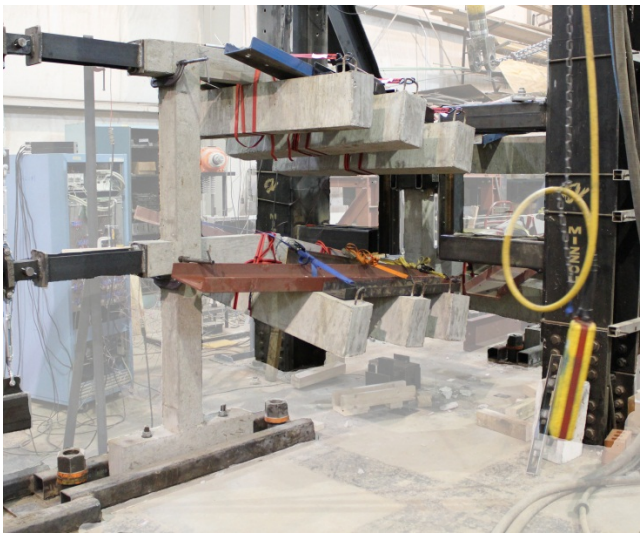

Figure 4.1.4: Failure after fourth drop

4.2 Dynamic Amplification Factors

Table **4.2.1** gives dynamic amplification factors for the horizontal loads and center displacements for each drop. The dynamic amplification factor is the ratio of the peak measured load or displacement to the residual load or displacement (the value when the frame stopped moving). The dynamic amplification factor shows the increase in the response due to the sudden application of the load. For the vertical deflection, the DAF was 1.08 for drop one, 1.11 for drop two, and 1.08 for drop three. These values are all relatively close, independent of the level of load, or damage to the frame. The horizontal displacement DAFs were also around 1.08, but increased to about 1.44 for the fourth drop. The increase in DAF was likely due to the transition from axial compression to axial tension as the frame went into catenary action. The load cell DAFs are much greater than those of the displacement values, with a value of 4.49 for the top load cell in drop three and average value of 2.0 for the top and bottom load cells in drop four. The DAF for the bottom load cell in drop three could not be determined because the residual

load was less than the noise in the load cell data ±0.45 kN (0.1 kip). The DAF for the third drop is higher than that of the fourth drop because the response of the third drop was still in the compressive arch range of response, and therefore stiffer than the fourth which went into catenary action. The high load cell DAFs are supported by DAF values from the strain gages on the reinforcement with values ranging from 1.7 to 5.1. The reason for high DAF values might be due to the shock of the sudden loading causing force in the connection before it has time to displace. Whatever the cause, this DAF needs careful consideration because excessive forces could lead to loss of the support connection and collapse of the frame.

Table 4.2.1: Dynamic amplification factors

	Drop 1	**Drop 2**	**Drop 3**	**Drop 4**
Vertical Disp.	-	1.08	1.11	1.08
Horiz. Disp. on top beam	-	1.09	1.04	1.44
Horiz. Disp. On bottom beam	-	1.10	1.09	1.46
Horiz. Load on bottom beam	-	-	-	4.49
Horiz. Load on top beam	-	-	1.82	2.18

4.3 Comparison of Test Data to Single Degree of Freedom Analysis

To gain a greater understanding of the effects of suddenly applying a load on the frame, a single degree of freedom (SDOF) analysis was undertaken. The reinforced concrete frame was reduced to a simple mass spring system using the approximate analysis procedures found in Biggs (1964).

The assumed mass of the model is equal to the sum of the masses of the beams, center column, and applied weights, all multiplied by a mass factor of 0.296. This mass factor represents the portion of mass contributing to the dynamics of the SDOF analysis. The applied load in the analysis is equal to the reaction from the instantaneously removed center column support. At time equal zero, this center support is assumed undamaged and provides a reaction force. Using static analysis of the frame conditions in the fourth drop, a point load is calculated which produces a maximum moment equivalent to that of the distributed weight in the test. This reaction force is equal to 12.6 kN (2.8 kips). The spring in the SDOF analysis is nonlinear and must simulate the behavior of the nonlinear force vs. deflection relationships found from the static tests in Stinger (2011) (refer to Figure **2.3.3**). An algorithm capable of accurately simulating such behavior was written based on the Central Difference Method. Strain rate effects must also be considered as they are potentially significant for a dynamic analysis (Iribarren et al., 2011). From the dynamic test, it was determined that the longitudinal reinforcement strain rate is approximately 0.004 strain/sec. According to the UFC 3-340-02 (2008), this would result in an increase in dynamic material strength of 1.04 for the steel and 1.10 for the concrete. The dynamic material strength factor for the concrete is applied in the compressive arch phase of response and the factor for steel is applied in the catenary action phase. Finally,

the resistance function was modified to account for the pre-existing damage in the specimen due to the initial drops.

The results of the SDOF analysis are shown in Figure **4.3.1**. As seen in the figure for the fourth drop, the peak displacement and period of the model correlate well with the empirical data. The peak force calculated in the spring at the maximum displacement is 30.7 kN (6.9 kips), corresponding to a force 2.4 times greater than the applied reaction force of 12.6 kN (2.8 kips). This shows that if a static analysis is performed, a dynamic increase factor of 2.4 must be applied to the load to simulate the dynamic response exhibited in this study.

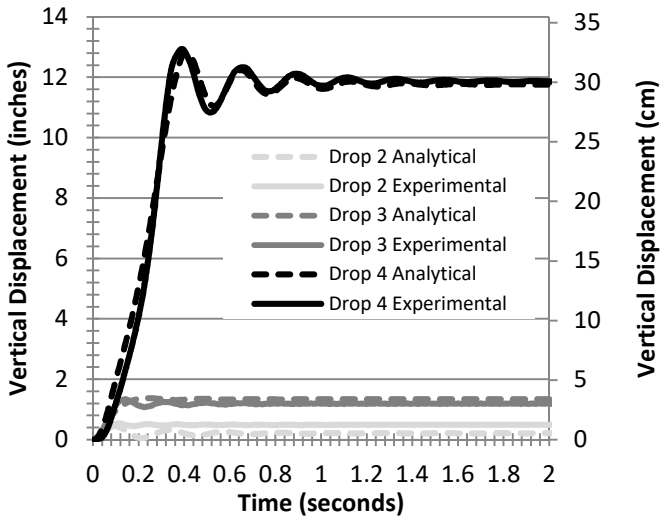

Figure 4.3.1: Results of SDOF analysis

A SDOF analysis was also conducted for load levels representative of the second and third drops, as well as load levels between the third and fourth drops. A graph of the results and test data is shown in Figure **4.3.1**. As seen in the graph, both the SDOF

analysis and empirical data show that the frame does not exceed the catenary action range of response in the second and third drops. However, when load is applied greater than that of the third drop, there is a very fine "tipping point" at which the SDOF analysis results in significant displacements. This "tipping point" represents the transition from the compressive arch phase to the catenary action phase, the results of which represent the snap-through effect.

Figure **4.3.2**, shows the results of the SDOF analysis in terms of peak displacement for increasing levels of applied force. The results show that if a force is applied which exceeds 10.85 kN (2.44 kip), it causes the frame to experience catenary action. To highlight this transition, consider the applied force value of 10.85 kN (2.44 kip), which results in a maximum displacement is 3.6 cm (1.42 in). However, for an applied force value of 10.89 kN (2.45 kip), the maximum displacement is 30.6 cm (12.06 in). This significant change in response illustrates the snap-through effect. At an applied force of 19.4 kN (4.36 kips) the frame exceeds its catenary action capability and collapses. This load corresponds to 66% of what would be required for collapse resistance.

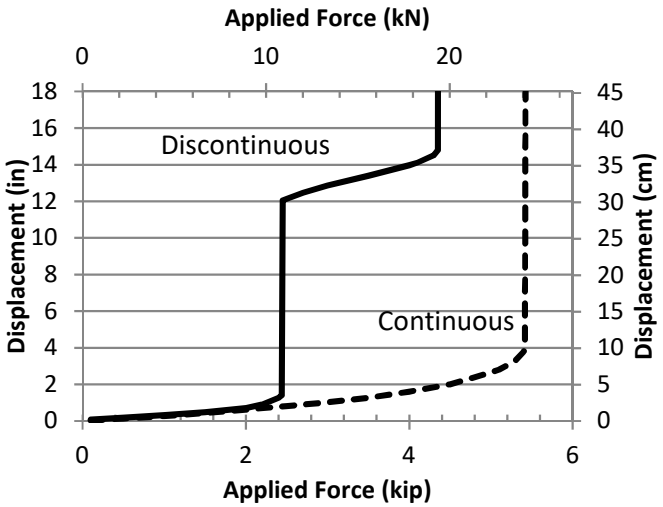

Figure 4.3.2: SDOF analysis with increasing applied force

A SDOF analysis was also conducted for the static test from Stinger (2011) involving the frame with continuous reinforcement. The results are shown in Figure **4.3.2**. In the case of a frame with continuous reinforcement, an applied force of 24.1 kN (5.4 kips) is required to cause the frame to reach the catenary action phase. Using the equivalent point load from the fourth drop of this study, a frame with continuous reinforcement would only exhibit a maximum deflection of 2.38 cm (0.94 in) and a maximum spring force of 19.3 kN (4.3 kips). This means that under the same load, the frame with continuous reinforcement would not enter the catenary action phase and all of the load would be resisted by flexural and compressive arch action. Regarding the load required for the frame with continuous reinforcement to enter the catenary action phase, this load corresponds to 81% of the 1.2*DL +0.5*LL load needed for collapse resistance. It is interesting to note that at this applied force, the deflection of the continuously reinforced frame would only be 9.82 cm (3.87 in). However, if a force is applied which exceeds 5.4 kips, the loss of support from flexural/compressive arch action is so severe that the frame

is unable to find equilibrium from catenary action. Hence, the ratio of flexural strength to catenary action strength is so close, that when the flexural/compressive arch strength is lost and the frame snaps through to the catenary action phase, there is not enough strength in the catenary phase to overcome the dynamic increase from the snap-through effect. The frame goes past the catenary action response and collapses. This is shown in Figure **4.3.2** by the infinite levels of displacement for applied loads of more than 5.4 kips. Therefore, for the case of continuous reinforcement, even though there is a catenary action phase of response under static loading, the frame is unable to utilize capacity from the resistance mechanism during a dynamic loading event.

For both reinforcement conditions, the DIF was calculated for increasing levels of applied load and plotted in Figure **4.3.3**. As seen in the figure, the DIF of the continuous frame gradually decreases from 2.0 to 1.08 as frame deforms and enters its inelastic response region. This agrees with the computational models presented in the previous section. After an applied load of 24.1 kN (5.4 kips) the frame experiences the snap-through effect and is unable to reestablish equilibrium, causing collapses. For the frame with discontinuous reinforcement, the DIF also decreases from 2.0 to a value of 1.09, at which point the frame has almost exhausted the flexural/compressive arch range of response. After an applied load of 10.36 kN (2.3 kip), the frame experiences the snap-through effect and the DIF increases to a value of 2.49.

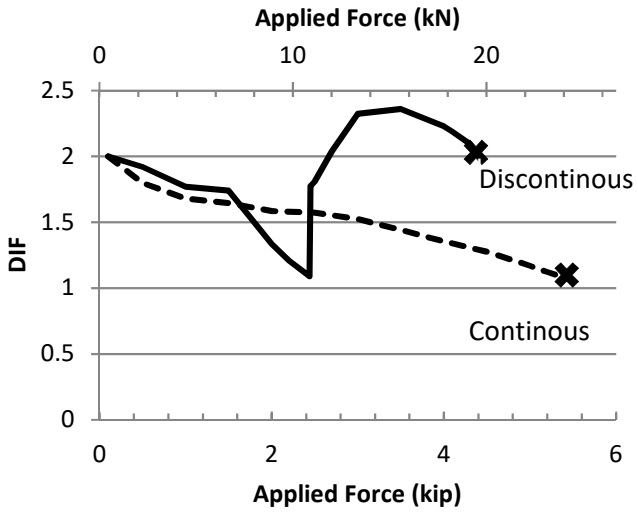

Figure 4.3.3: DIFs from SDOF analysis

5 FURTHER RESEARCH

The results presented in this paper are based on the testing of a single frame. Although this study does provide valuable insight into the inertial effects from a disproportionate collapse, additional testing and analysis on multiple frames will provide a larger sample and therefore eliminate possible outlier results. Also, an effect which resulted from the use of a single frame was the softening of the beams because of multiple drops. Although softening primarily affects Vierendeel Action, its effect on the dynamic study must be accounted for. Furthermore, an analytical study performed by Brunesi et al. (2015) determined that secondary beams and floor slab continuity significantly contribute to the disproportionate collapse resistance of reinforced concrete buildings. These factors were not accounted for in the dynamic test, and an empirical evaluation of their contribution would provide valuable insight. Finally, the local effects of an event that would cause a disproportionate collapse, such as an explosion and the energy imparted to the structure, require consideration. These variables warrant further research.

6 SUMMARY AND CONCLUSION

This paper presents the results from four dynamic tests of a reinforced concrete frame with discontinuous reinforcement under various levels of applied load. The first three drops were not sufficient to surpass the compressive arch action range of response. The forth drop, with a load corresponding to 42% of the 1.2*DL + 0.5*LL design load specified by modern guidelines, resulted in a catenary action range of response. Analysis of the test data from all drops showed a consistent dynamic amplification factor for the vertical deflection of about 1.09. The dynamic amplification factors for the horizontal load and reinforcement strain were much greater, as much as 4.49, possibly due to a shock effect of the dynamic loading.

A SDOF analysis was conducted and shown capable of replicating the experimental results. The results from the SDOF analysis were used to evaluate the dynamic increase factors (load felt in structure/applied load) at various levels of applied load. The results show that there is a very fine tipping point at which the structure is pushed past the compressive arch or flexural range of response into the catenary action range of response. Due to this snap-through effect, the DIF increases significantly and can be as great as 2.4. It is interesting to note that the SDOF analysis of a frame with discontinuous reinforcement showed that the frame reached equilibrium during the catenary action range of response. However, the analysis of a frame with continuous reinforcement showed that the frame was pushed past the catenary range of response and collapsed.

Based on the experimental data and analytical analysis, the conclusions of this research are:

- A frame with discontinuous reinforcement was dynamically tested and able to support 42% of the 1.2*DL + 0.5*LL design load specified by modern guidelines due to catenary action. This results in an effective DIF equal to 2.4. This result is supported by a SDOF analysis conducted using the results from this test and a "sister" static test (Stinger, 2011). The SDOF analysis showed that the discontinuously reinforced frame would experience near identical deflections with an applied force equal to 2.4 times the equivalent point load, or in other words with an effective DIF equal to 2.4. The SDOF analysis also showed that at 66% of the design load, the frame would exceed the catenary action phase and fail. This is a significant level of load, and therefore shows the inherent collapse resistance of reinforced concrete frames. Furthermore, because the two-dimensional frame in this study did not consider continuity from floor slabs or secondary beams, these results may be conservative. The inclusion of continuity may exhibit even greater disproportionate collapse resistance and therefore result in a lower DIF.
- There is a snap-through effect when the frame loses compressive arch action and flexural resistance and enters the catenary action range of resistance. This transition between resistance mechanisms causes a sharp increase in the dynamic increase factor causing it to exceed the value of 2.0 commonly specified by modern guidelines.

REFERENCES

American Concrete Institute. (2008). "Building Code Requirements for Structural Concrete (318-05)." Farmington Hills, MI.

Bazan, M.L. (2008). "Response of Reinforced Concrete Elements and Structures Following Loss of Load Bearing Elements." Dissertation, Northeastern University, MA.

Biggs, J. (1964). "Introduction to Structural Dynamics." McGraw-Hill Book Company, NY.

Brunesi, E., Nascimbene, R., Parisi, F. and Augenti, N. (2015). "Progressive collapse fragility of reinforced concrete framed structures through incremental dynamic analysis." *Engineering Structures*, 104, pp. 65-79.

Byfield, M., Mudalige, W., Morison, C., and Stoddart, E. (2013). "A review of progressive collapse research and regulations." Institution of Civil Engineers (ICE), Vol. 167 Issue SB8, pp. 447-456.

Corley, W., Mlakar, P., Sozen, M. and Thornton, C. (1998). "The Oklahoma City bombing: summary and recommendations for multihazard mitigation." *Journal of Performance of Constructed Facilities*, 12(3), pp. 100-112.

Couwenberg, R. (2013). "Progressive Collapse of Reinforced Concrete Structures." Master Thesis, Technische Universiteit Eindhoven, Eindhoven, Netherlands.

Department of Defense (DOD). (2009). "Design of Buildings to Resist Progressive Collapse." Unified Facilities Criteria (UFC) 4-023-03, July 2009.

Ernsberger, R. Jr., (2016). "1983 Beirut Barracks Bombing: 'The BLT Building Is Gone!'" HistoryNet, Oct 2016.

General Services Administration (GSA). (2003). "Progressive Collapse Analysis and Design Guidelines." General Services Administration, June 2003.

Gudmundsson, G., and Izzuddin, B. (2010). "The 'sudden column loss' idealization for disproportionate collapse assessment." *The Structural Engineer*, Vol. 88 Issue 6.

He, G., and Yi, W. (2008). "Experimental Study on Collapse-Resistant Behavior of RC Beam-Column Sub-Structure considering Catenary Action." The 14th World Conference on Earthquake Engineering, October 2008 Beijing, China.

Iribarren, S., Berke, P., Bouillard, P. Vantomme, J., and Massart, T. (2011). "Investigation of the influence of design and material parameters in the progressive collapse analysis of RC structures." *Engineering Structures*, V 33, pp. 2805 – 2820.

Jenkins, J. (2001). "Oklahoma City bombing." Encyclopedia Britannica. <https://www.britannica.com/event/Oklahoma-City-bombing>.

Kirk, J. (2005). "The World Trade Center Collapse: Analysis and Recommendations." Massachusetts Institute of Technology. Department of Civil and Environmental Engineering. <http://hdl.handle.net/1721.1/31114>.

Marjanishvili, S., and Agnew, E. (2006). "Comparison of Various Procedures for Progressive Collapse Analysis." *Journal of Performance of Constructed Facilities*, 20(4), November 2008, pp. 365-375.

Martin, R., and Delatte, N. (2000). "Another Look at the L' Ambiance Plaza Collapse." *Journal of Performance of Constructed Facilities*, 14(4), pp. 160-165.

McKay, A., Marchand, K., Williamson, E., Crowder, B., and Stevens, D. (2007). "Dynamic and Nonlinear Load Increase factors for Collapse Design and Analysis." Proc., Int. Symp. on Interaction of the Effects of Munitions with Structures (ISIEMS) 12.1, Orlando, FL.

McKee, C. (2010). "The titling south tower gives it away." Truth and Shadows. <https://truthandshadows.wordpress.com/2010/11/>.

National Institute of Standard and Technology (NIST). (2007). "Best Practices for Reducing the Potential for Progressive Collapse in Buildings." NISTIR 7396, February 2007.

Orton, S. (2007). "Development of a CFRP System to Provide Continuity in Existing Reinforced Concrete Buildings Vulnerable to Progressive Collapse." Dissertation, 2007.

Orton, S., Jirsa, J., and Bayrak, O. (2009). "Carbon Fiber-Reinforced Polymer for Continuity in Existing Reinforced Concrete Buildings Vulnerable to Collapse." *ACI Structural Journal*, 106 (5), pp. 608-616.

Pearson, C., and Delatte, N. (2005). "Ronan Point apartment tower collapse and its effect on building codes." *Journal of Performance of Constructed Facilities*, Vol. 19, No. 2, May 2005.

Poisson, C. (2012). "Photos: L' Ambiance Plaza Collapse. Hartford Courant. <http://www.courant.com/business/hc-lambiance-plaza-anniversary-photos-20120404-photogallery.html>.

Progressive Collapse Resistance Competition. (2007). <http://www.pcrc2007.neu.edu>.

Regan, P. (1975). "Catenary Action in Damaged Concrete Structures." *Industrialization in Concrete Building Construction ACI SP-48*, pp. 191-225.

Ruth, P., Marchand, K., and Williamson, E. (2006). "Static Equivalency in Progressive Collapse Alternate Path Analysis: Reducing Conservatism While Retaining Structural Integrity." *Journal of Performance of Constructed Facilities*, 20(4), pp. 349-364.

Sasani, M., Bazan, M., and Sagiroglu, S. (2007). "Experimental and Analytical Progressive Collapse Evaluation of Actual Reinforced Concrete Structures." *ACI Structural Journal*, 104(6), Nov-Dec 2007, pp. 731-739.

Sasani, M., and Sagiroglu, S. (2008a). "Progressive Collapse of Reinforced Concrete Structures: A Multihazard Perspective." *ACI Structural Journal*, 105(1), January-February 2008, pp. 96-103.

Sasani, M., and Sagiroglu, S. (2008b). "Progressive Collapse Resistance of Hotel San Diego." *Journal of Structural Engineering*, 134(4), March 2008, pp. 478-488.

Sasani, M., and Sagirgoglu, S. (2010). "Gravity Load Redistribution and Progressive Collapse Resistance of 20-Story Concrete Structure Following Loss of Interior Column." *ACI Structural Journal*, V. 107, No. 6, Nov-Dec. 2010, pp. 636-644.

Schellhammer, J., Delatte, N., and Bosela, P. (2013). "Another Look at the Collapse of Skyline Plaza at Bailey's Crossroads, Virginia." *Journal of Performance of Constructed Facilities*, 27(3), pp. 354-361.

Smilowitz, R. (2006). "Progressive Collapse: Emerging Challenges for the Design Professional." *Journal of Performance of Constructed Facilities*, 20(4), November 2008, pp. 307-308.

Stinger, S. (2011). "Evaluation of Alternative Resistance Mechanisms for Progressive Collapse." Master Thesis, University of Missouri Columbia, Columbia, MO.

Su, Y., Tian, Y., and Song, X. (2009). "Progressive Collapse Resistance of Axially-Restrained Frame Beams." *ACI Structural Journal*, 106 (5), pp. 600-607.

Tian, Y., and Su, Y. (2011). "Dynamic Response of Reinforced Concrete Beams Following Instantaneous Removal of a Bearing Column." *International Journal of Concrete Structures and Materials*, Vol 5, No. 1, pp. 19-28.

Tsai, M. (2011). "Analytical Load and Dynamic Increase Factors for Progressive Collapse Analysis of Building Frames." Proceedings of the AEI 2011 Conference.

Yi, W., He, Q., Xiao, Y., and Kunnath, S. (2008). “Experimental Study on Progressive Collapse-Resistant Behavior of Reinforced Concrete Frame Structures.” *ACI Structural Journal*, V.105, No.4, July-August 2008, pp. 433-439.